Robotic feet modeled after ungulates improve locomotion on soft wet grounds

IOP Publishing Bioinspir. Biomim. 19 (2024) 066009 https://doi.org/10.1088/1748-3190/ad839c

Bioinspiration & Biomimetics

CrossMark

RECEIVED
6 July 2024

REVISED
16 September 2024

ACCEPTED FOR PUBLICATION
4 October 2024

PUBLISHED
4 November 2024

PAPER

Robotic feet modeled after ungulates improve locomotion on soft wet grounds

S Godon*, A Ristolainen and M Kruusmaa

Centre for Biorobotics, School of IT, Department of Computer systems, Tallinn University of Technology (Taltech), Tallinn, Estonia
* Author to whom any correspondence should be addressed.

E-mail: simon.godon@taltech.ee

Keywords: animal leg, foot, bioinspiration, mud, soft yielding ground, quadruped robot

Abstract

Locomotion on soft yielding grounds is more complicated and energetically demanding than on hard ground. Wet soft ground (such as mud or snow) is a particularly difficult substance because it dissipates energy when stepping and resists extrusion of the foot. Sinkage in mud forces walkers to make higher steps, thus, to spend more energy. Yet wet yielding terrains are part of the habitat of numerous even-toed ungulates (large mammals with split hooves). We hypothesized that split hooves provide an advantage on wet grounds and investigated the behavior of moose legs on a test rig. We found that split hooves of a moose reduce suction force at extrusion but could not find conclusive evidence that the hoof reduces sinkage. We then continued by designing artificial feet equipped with split-hoof-inspired protuberances and testing them under different conditions. These bio-inspired feet demonstrate an anisotropic behavior enabling reduction of sinkage depth up to 46.3%, suction force by 47.6%, and energy cost of stepping on mud by up to 70.4%. Finally, we mounted these artificial feet on a Go1 quadruped robot moving in mud and observed 38.7% reduction of the mechanical cost of transport and 55.0% increase of speed. Those results help us understand the physics of mud locomotion of animals and design better robots moving on wet terrains. We did not find any disadvantages of the split-hooves-inspired design on hard ground, which suggests that redesigning the feet of quadruped robots improves their overall versatility and efficiency on natural terrains.

1. Introduction

Legged robots present an interesting blend of agility, versatility, and endurance, making them suitable for tasks in natural environments [1–3]. Among those environments, soft yielding grounds, deforming under the robot's weight, are particularly challenging to access [4]. Locomotion on yielding grounds is researched heavily in terramechanics [5]. This research field, however, which addresses locomotion on natural yielding grounds from a traction perspective, focuses on the shearing forces of wheeled or tracked vehicles. Compared to locomotion using wheels or tracks, legged locomotion on yielding grounds is mainly challenged by leg sinkage, leg extrusion force, and stability [4, 6–8].

In the past 20 years, some research started to address the physics of interactions between moving robots and deformable grounds, with an emphasis on granular media [9–17]. With the recent advances in quadruped robotics, works addressing quadruped locomotion on soft ground started to appear, with focus on control [18–24], leg or foot design [25–30], both [31, 32], or ground properties estimation [22, 30].

However, little work has addressed locomotion on mud or other soft wet grounds (e.g. wet snow). These grounds are different from dry granular media because they have a behavior that depends on the rate of stress and the direction of stress, they deform under load but do not recover: they are called viscoplastic. The few works in this domain address the characterization and modeling of mud behavior under vertical loads [6, 7] or robot models to address different characteristics of the mud behavior such as the effects of mud water content on flipper-driven locomotion, leg compliance, or rotation speed and shape of elliptic rotating legs [33–35]. Even fewer addressed

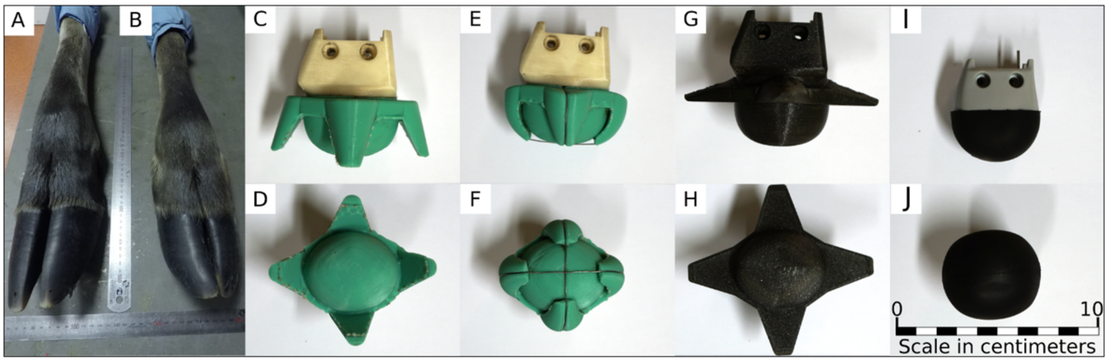

Figure 1. The moose legs and the four different synthetic feet tested. (A) Moose front leg, (B) Moose hind leg. (C), (D) The proposed bio-inspired anisotropic foot. (E), (F) The proposed bio-inspired foot with fastened digits. (G), (H) A foot with rigid extended digits. (I), (J) The commercial Go1 foot. Figures (C)–(J) are at the same scale, displayed in (J).

quadruped locomotion in shallow mud [18, 36], and only our own previous work addressed quadruped locomotion in deep mud [8].

Yet, muddy fields are ubiquitous. Sea shores, lake banks and riverbanks, snow, wetland, marshes or wet forests, are examples of lands that are inaccessible to legged robots. In our previous research [8], we demonstrated a quadruped controller for wading in muddy fields and showed that using a static walking gait and estimating extrusion forces based on sensor signals reduced energy consumption and increased speed.

However, the physics of interaction with soft wet grounds is complex and controller design is limited by the hardware of the robot. This work is inspired by the observation that many large ungulates, living also in wet terrains have split hooves in the front of their feet and two back digits a few centimeters above the ground at the back of their feet (even-toed ungulates). There does not seem to be biology research investigating ungulate locomotion on wet ground besides a work studying cow step length and speed in excrata [37]. Some robot research suggest that the split hooves provide stability and added traction in accidented terrains [26, 38]. However, we hypothesize that they also enable to improve locomotion performance on yielding terrains, such as mud or sand because their anisotropic motion makes them expand at intrusion into the ground and contract at extrusion. This should lead to reduced sinkage and suction force when pulling out the leg, both leading to reduced energy consumption of walking. Total energy spent is an indicator of the cost of traversing, and thereby the endurance.

Therefore, our hypothesis that split hooves improve motion on yielding terrains can be decomposed into three hypotheses: (I) split hooves enable to reduce sinkage in muddy terrains, (II) split hooves enable to reduce suction force in muddy terrains, (III) split hooves enable to save energy for moving in muddy terrains.

To answer our research questions, we first conducted rig experiments using moose feet (figures 1(A) and (B)), an even-toed ungulate living in wet areas and snow, and then designed a synthetic foot (figures 1(C) and (D)) inspired by the split hooves' characteristics, which we compared to three reduced versions of the foot (figures 1(E)–(J)). Finally, we mounted our bio-inspired feet on a Go1 quadruped robot traversing a muddy track.

2. Materials and methods

2.1. Preliminary rig experiments with moose feet

The moose legs were obtained from a local hunting association, the legs were dissected and held in cold but above freezing temperature for 48 h while the experimental rig was prepared. The experiments lasted approximately 5 h. We performed two types of experiments for each leg: digits free and digits fastened. To fasten the digits, we used zip ties and steel wire to bind the digits together. The amount of water in the mud was dictated by the setup: the mud had to be soft enough to enable all four toes to be submerged, but also hard enough so the maximum force could be reached within the range of motion of our actuator, i.e. 30 cm. We could therefore test only one water content, i.e. $R_w = 0.34$. The ratio of water to solid matter in the mud R_w was computed according to the following formula, where M_w is the mass of water, and M_{ds} the mass of dry soil:

$$R_w = \frac{M_w}{M_{ds}}.$$

The experimental setup can be observed in figure 2(A). On the top of a rigid frame, is mounted a 30 cm range linear actuator (Moteck LD3-24-40-E6-300), to which the feet were attached. The linear actuator provides position feedback at 150 Hz. On the bottom part of the rigid frame, a Force/Torque sensor (ATI Axia80-M20) records force at a rate of 150 Hz.

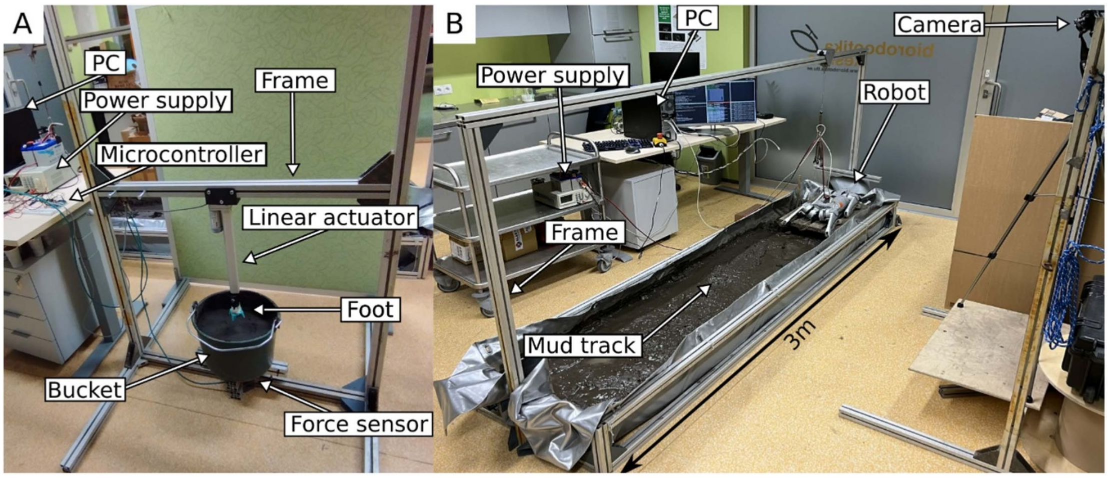

Figure 2. The two experimental setups used in this research. (A): Linear test rig. It consists of a frame on which are mounted a linear actuator on the upper part, and a force sensor on the lower part. On the linear actuator are mounted the different feet to test. On top of the force sensor is positioned a bucket of soil. The low-level control of the motor is performed on a microcontroller, and the power comes from an external power supply. High-level commands and recording of force and position are done from an external computer using ROS. (B) A track filled with mud on which a Go1 quadruped robot walks. The robot is secured by a trolley freely following the robot and attached to it with steel cables. The track contains a 3 m × 0.8 m × 0.12 m volume of mud. High-level control of the robot and data recording is done through an external computer using ROS. Power comes from an external battery connected to a power supply to enable longer runtime and to insert an emergency stop in the power circuit. A camera records the scene to measure the robot's position.

For each experiment, a 300 N target force was given, and the rig went down until the target force was reached, at a controlled constant speed of 5.5 mm s^{-1} (which was the maximum speed reachable by the actuator).

The low-level control of the motor was implemented using a microcontroller, and high-level commands and data recording were implemented using the robot operating system (ROS). The power was provided to the motor by an external power supply unit.

The tests were conducted for the two different digit configurations described above, for two different legs, and repeated ten times, resulting in 2 × 2 × 10 experiments.

For processing the data, we filtered both the position and force curves, and offset them so the contact range would start when the recorded force was above a 1 N threshold. We then computed the work W using the following equation, where z_i is the depth from the mud surface, F_i is force, and $\mathrm{n_f}$ is the final timestep:

$$W = \sum_{n=1}^{n_f} F_n \left(z_n - z_{n-1}\right).$$

Further, we calculated the components of the total work: the positive downward work of pushing the foot down until the target force was reached, the negative work representing the recoverable elastic energy when the foot is lifted, and the positive upward work, representing the energy spent to withdraw the leg from the substrate.

2.2. Design of bio-inspired feet and rig experiments

Taking inspiration from the ungulates' digits, we designed a silicone (Elite double 22 from Zhermack) foot consisting of the same shape as the original Go1 ball foot (see figures 1(I) and (J)) and added deformable digits on its periphery (figures 1(C) and (D)). The material was chosen because of its ease of use and because of the promising results obtained using this material in our previous research [6]. The shape of the digits results from mimicking the conic structure of the digits. The width of the digits, and thereby the radial stiffness was determined in an iterative process involving finite element method (FEM) analysis and rapid prototyping followed by manual testing of the feet in mud with varying properties while making sure that they provide significant resistance to sinkage. Figure 3 shows the FEM model of the final version of the foot when subjected to a 60 N upward force, to simulate the intrusion phase of the foot into mud (A), and when subjected to a 30 N downward force (half of the maximum sinking force [6]), to simulate the extrusion phase of the foot (B). The FEM was conducted in ®Solidworks using a hyperelastic model, with the data from the tensile tests performed in [39] for the material properties. The model was constrained with a fixed support on the top surface, where the leg is fixed. For the intrusion phase, force was defined as a uniform pressure on all down-facing surfaces. For the extrusion phase, force was split evenly between a negative pressure on the down-facing surfaces, representing suction force, and a positive pressure on the up-facing surfaces, representing the weight of mud on top of the foot. The proposed final design of the

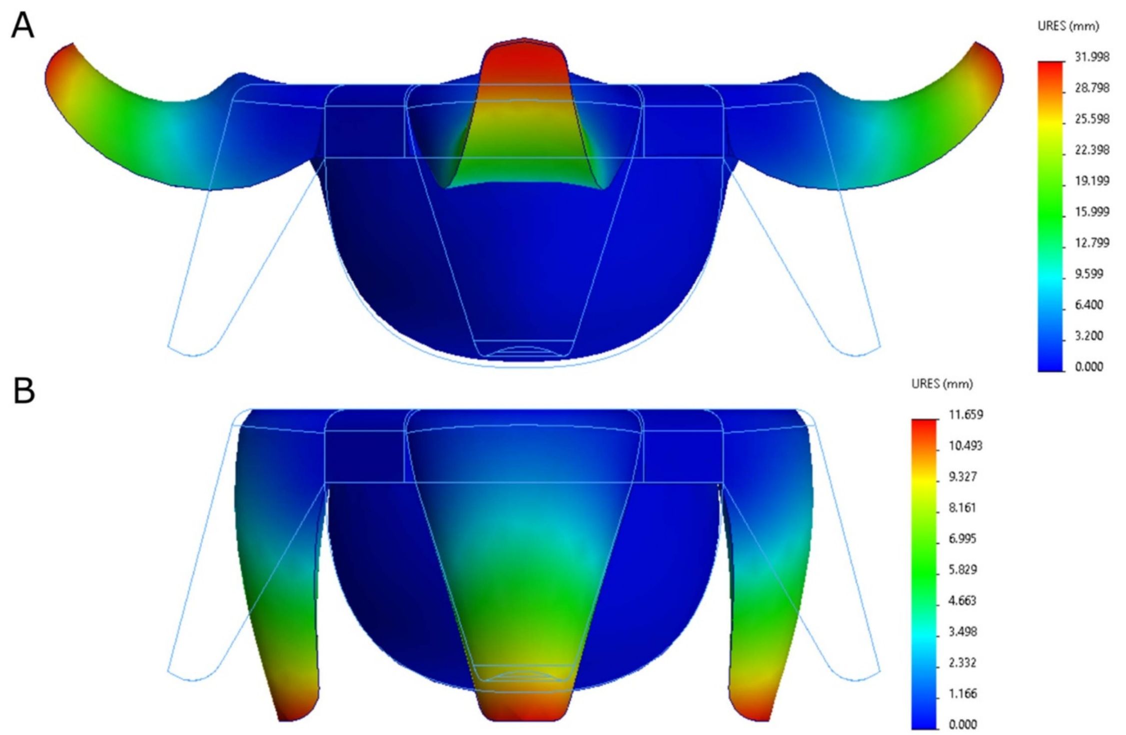

Figure 3. Finite element method of the proposed foot. (A): Resultant displacement (mm) of the foot when subject to a vertical upward force of 60 N, simulating the intrusion phase of the foot into mud. The red parts show the maximum displacement (32 mm), and the blue part the minimum (0 mm). The simulation shows that when subjected to a 60 N upward force, the digits fully extend passively. The light blue lines represent the shape of the undeformed foot. (B) Resultant displacement (mm) of the foot when subjected to a 30 N downward force, simulating the extrusion phase of the foot. The red parts show the maximum displacement (11.7 mm) and the blue regions show the minimum displacement (0 mm). The simulation shows that when subjected to a 30 N downward force, the foot digits retract passively. The light blue lines represent the shape of the undeformed foot.

foot enables it to passively, fully extend, and retract its digits to increase sinkage resistance and reduce suction force, respectively. A fabric mesh was cast inside the lower part of the foot to resist tearing, and a rigid kernel was placed at the center of the mold to provide a strong anchor point for the screw during the assembly with the leg.

The experimental setup for synthetic legs and moose legs was the same, see figure 2(A). For artificial feet experiments, the force and position were recorded in the same way as in the animal's feet experiments. However, thanks to the smaller dimensions of our bio-inspired feet, we could test different water contents of the mud without being limited by the dimensions of the experimental setup.

The water contents tested are 0.21, 0.25 and 0.27, which are three values selected in the region where the behavior of mud varies significantly depending on the water content. Below 0.2, the behavior of mud remains relatively constant, while after 0.27, the mud has a very low stiffness and would not support the load within the range of the target force [6]. The target force for the artificial feet was selected so it would be later comparable with the experiments with the Go1 robot. We experimentally established that with the controller used for the Go1 experiments, the maximum force on a single foot was 60 N, or half of the robot's weight. Therefore, for the rig experiments on the four different feet, we set a target force command of 60 N.

The experiments were conducted with specimens on figures 1(C)–(J). with each specimen, the experiment was performed 10 times under each mud consistency (this accounts for $4 \times 10 \times 3$ experiments altogether). Data processing was identical to what was described for the moose feet experiments.

2.3. Experiments on a quadruped robot

The robot experiments with GO1 were conducted with a controller developed and tested in our previous research [8]. The controller was specially developed for walking in deep mud, and it was established in [8] that the commercially available foot of GO1 does not allow walking in deep mud (the robot gets stuck and falls).

The controller developed in [8] is based on a tripod static gait, which places the body in a stable position based on the estimated ground properties, measured and modeled during the intrusion phase of the leg. In this controller design, the inputs—leg sequence, step length and height, swing duration, clearance, and stance width—are kept constant throughout the experiment. The controller is designed to minimize excessive suction forces by slowing leg movement while it is in mud and shifting the robot's center of mass further from the leg when high suction forces are anticipated, thus preventing the robot from toppling. These two features, combined with the bio-inspired artificial feet's reduced sinkage, account for the differences in speed and mechanical cost of transport (MCoT) observed in the results section. The controller remains the same across all three sets of experiments, with varying results arising from differences in sinkage depth and suction force between the two sets of feet or ground stiffness. For more details on the controller, we refer interested readers to [8].

The setup of the robot experiment is shown in figure 2(B). The robot was walking on a 12 cm deep muddy track and secured by a freely rolling trolley suspended above the robot (for safety and for the convenience of using an external power source). High-level commands and data recording were performed using ROS software on an external computer for simplicity. The experiments were also video recorded to track the distance covered by the robot. The videos were post-processed using the ®Kinovea software. The MCoT of the robot was computed during post-processing by summing up the mechanical output of all motors for the entire experiments. The contribution of each motor was calculated with the following formula:

$$W_i = \sum_{n=0}^{n_f} \tau_i(n)\,\omega_i(n)$$

where n represents the timestep, n_f the last timestep of the experiment, τ_i the estimated torque of the motor i, and ω_i the estimated rotational velocity of the motor i. ω_i and τ_i are directly available from motor feedback. Only the positive work is computed, the negative work is not subtracted from the result because negative work is not practically recovered.

The MCoT was then computed using the following formula:

$$\mathrm{MCoT} = \frac{E}{\mathrm{mgd}}.$$

Where E is the total mechanical energy spent, computed by summing the individual works from all motors W_i, $m = 12$ kg is the mass of the robot, $g = 9.81$ m s^{-2} is gravitational acceleration, and d is the distance covered by the robot, measured from video recording using the ®Kinovea software.

The soil had a water content of 0.25 which is the same water content as for the rig experiment. That allowed us to later establish that the energy saving for the robot and isolated foot experiments were consistent with each other.

Three different experiments were performed:

- Using the original Go1 robot feet in mud, which served as a baseline
- Using the original Go1 feet on hard ground, to compute the MCoT in the absence of mud and therefore compare the contribution of our feet to the mud-related part of the MCoT.
- Using our bio-inspired anisotropic feet

3. Results

3.1. Moose leg experimental results

The first experiments were performed on moose legs, one front leg (figure 1(A)), and one hind leg (figure 1(B)) in two conditions: the digits fastened to the foot and the digits allowed to move freely. The results of the experiments performed on moose feet can be observed in figure 4. Figure 4(A) shows the four phases of work for each condition and for each leg. Figure 4(B) shows the depth reached during the intrusion phase for the four test conditions. Figure 4(C) presents the maximum suction force reached while pulling the leg out of the mud after the step for a hind leg and a front leg. The results are consistent for both the hind and front legs of the moose with respectively 8.4% (p-value < 0.01) and 4.3% (p-value < 0.01) increase in suction force when the digits are fastened. However, the sinkage is not statistically (for the hind leg) or in absolute value different for both legs (26.9 cm vs 26.8 cm for the front leg, p-value < 0.01, and 25.8 cm vs 25.9 cm for the hind leg, p-value > 0.8). The work spent in mud deformation is also similar for both front and hind legs (18.03 J vs 17.86 J for the front leg, p-value > 0.7, and 13.93 J vs 14.14 J for the hind leg, p-value > 0.4).

3.2. Proposed bio-inspired anisotropic foot

The proposed anisotropic foot design can be observed in figures 1(C) and (D). To make experiments comparable, it is designed based on the original foot of the Go1 robot (figures 1(I) and (J)) and similar to other commonly available quadruped commercial robots. Our proposed design is achieved by adding passive appendices expected to serve the functionality of ungulate toes (figures 1(A) and (B)). The passive silicone appendices expand and retract as force is applied during intrusion and extrusion. The manufacturing is simple, and it resists tearing thanks to an embedded fabric mesh. A rigid fastener is used to fasten the foot to the robot with screws. Additionally, we proposed two variations for comparative experiments: a bio-inspired foot with fastened digits (figures 1(E) and (F)) and rigid extended digits (figures 1(G) and (H)).

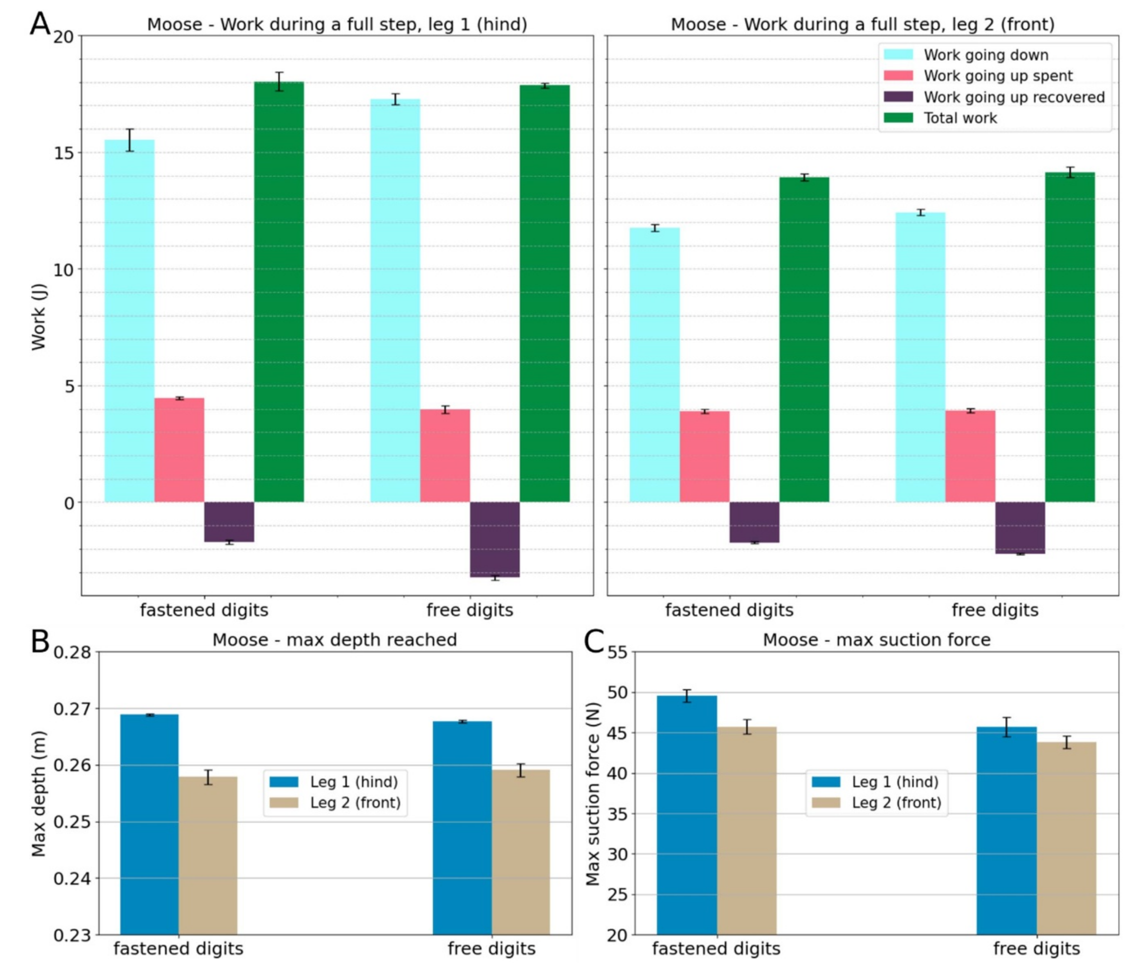

Figure 4. Experimental results for the moose feet experiments. This figure illustrates the three metrics tested for both the front and hind legs, with fastened or free digits. It demonstrates the similar behavior of the front and hind legs for all the parameters tested and indicates a difference between fastened and free digits in the suction force. (A) Work during the different stages of the step (B) Maximum depth reached during intrusion of the leg (C) Maximum suction force during pullout of the leg. Each of the bars represents the median of a series of 10 samples, and the error bars represent their standard error.

3.3. 1D test results in soft ground

Figure 5 presents the results obtained in the rig experiments using the synthetic feet with three different water contents. Figure 5(A) shows that compared to the original Go1 foot, the proposed foot enables lowering the energy spent for ground deformation, by 19.1% (p-value < 0.01), 70.4% (p-value < 0.01), and 40.3% (p-value < 0.01) respectively for the low, medium and high water contents. The rigid extended foot demonstrates an even higher energy saving of 82.4% (p-value < 0.01) on the medium water content condition, mainly gained from the intrusion phase, because the foot sinks less (figure 5(B)) due to its already fully extended digits, while it takes a few millimeters for the bio-inspired foot to expand them. Sinkage depth is also reduced in low, medium and higher water content conditions, with a 18.4% (p-value < 0.01), 46.3% (p-value < 0.01) and 37.4% (p-value < 0.01) sinkage depth reduction, respectively. In the very wet condition, the anisotropic design of the bio-inspired foot demonstrates its ability to reduce the suction force (figure 5(C)). It reduces it by 82.1% (p-value < 0.03), 47.6% (p-value < 0.01) and 21.0% (p-value < 0.01) compared to the original Go1 foot in the least, medium and wettest conditions, respectively. The rigid extended foot here demonstrates that simply increasing the foot surface, without anisotropic feature is impeding locomotion, with an increase of 71.1% (p-value < 0.01) in the suction force in the wettest condition compared to the bio-inspired anisotropic foot.

Figure 6 shows typical curves observed in the wettest condition. This condition was chosen because it is the one that best demonstrates the contributions of all the features present in the different feet. Figure 6(A) shows the force vs depth curves for the four different tested feet. The graph reads in the clockwise direction, i.e. the force and sinkage both increase up to the target force, then the depth starts to decrease (foot withdrawing). The withdrawing causes the force to decrease (elasticity) and then to quickly become negative due to the suction force, until the suction

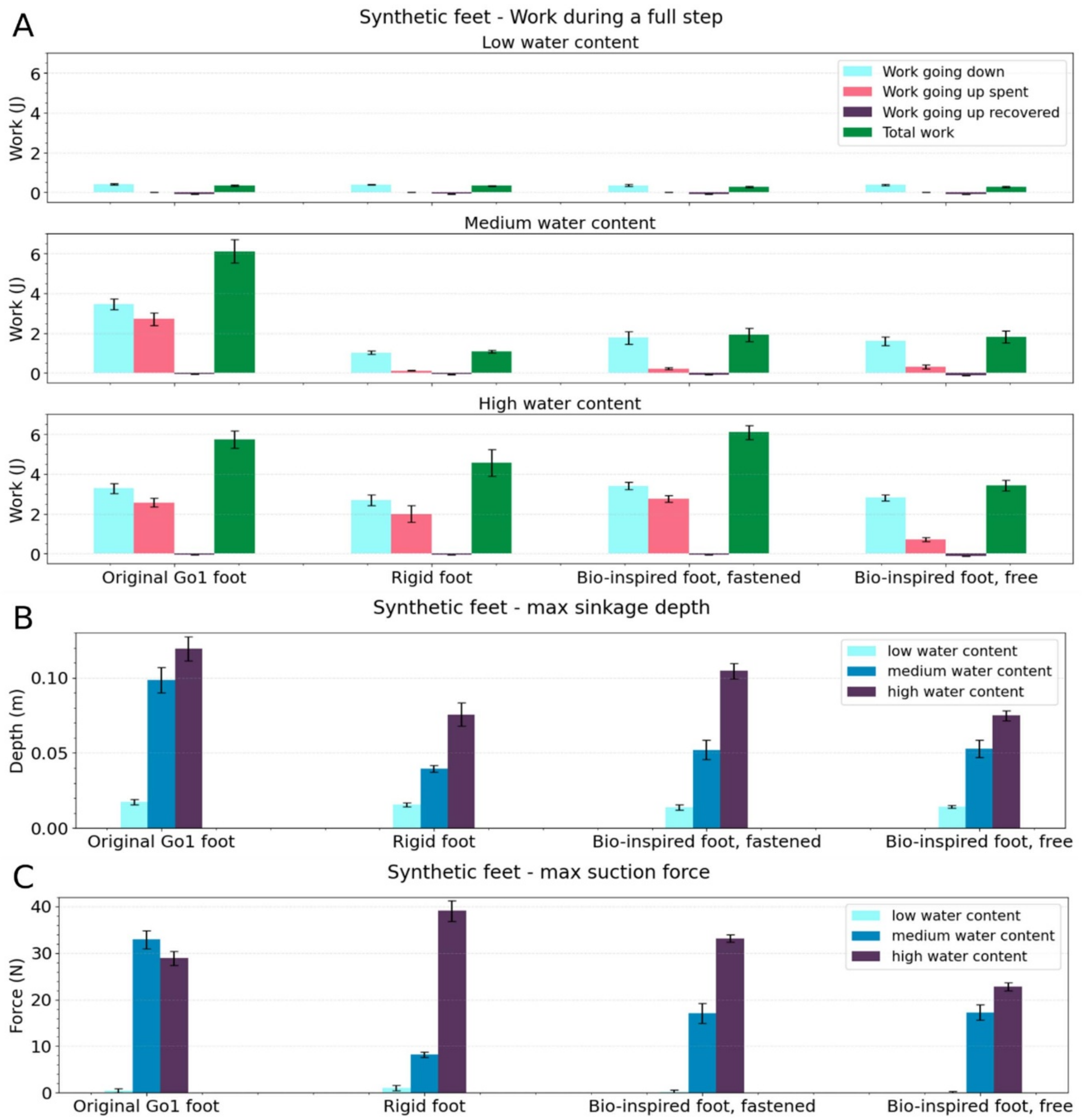

Figure 5. Experimental results of the linear rig tests performed using the four synthetic feet on muds with three different water contents. This graph illustrates how each foot's behavior varies with the water content, and for each water content, the three metrics we compare per foot. (A) Work during an entire step, including the positive work exerted when pushing down, the positive work from withdrawing the foot from the mud, and the negative work from elastic energy stored in the foot. Each graph summarizes results from a different water content. (B) The maximum depth reached by all the synthetic feet given the input force command. (C) The maximum suction force during the withdrawal phase of the step, after the target force was reached. Each of the bars represents the median of a series of 10 samples, and the error bars represent their standard error.

is released, and the force returns to zero. The area covered by the loop represents the work exerted by the foot on the mud. Figure 6(B) shows the force vs time curve. This curve allows to compare the speed at which the different feet reach the target force or release the suction.

Figure 7 shows timeshots of the robot traversing the track using the original Go1 feet, the bio-inspired anisotropic feet, and as a comparison, on hard ground using the original Go1 feet.

Figure 8 shows the performances of the quadruped robot on the track in the three test conditions. On the left (figure 8(A)), the MCoT is depicted. The MCoT using the original Go1 feet is 2.42, which is slightly higher than the 2.12 measured in our previous research [8], where the experiments were performed with $R_w = 0.35$, i.e. a thinner and less sticky mud. Compared to using the original Go1 feet, the bio-inspired feet lead to a 38.7% (p-value < 0.01) energy saving. If we deduct the base cost of transport from this, i.e. the cost of transport on hard ground (0.736), we end up with a contribution of mud to the MCoT of 1.680 with the original Go1 feet, and 0.749 with the bio-inspired feet. Therefore, for the component of MCoT which is due to mud, the bio-inspired feet help to save 55.6% of the energy which is coherent with the 40.2%–70.3% observed in the 1D rig experiments. Figure 8(B) shows that the speed of the

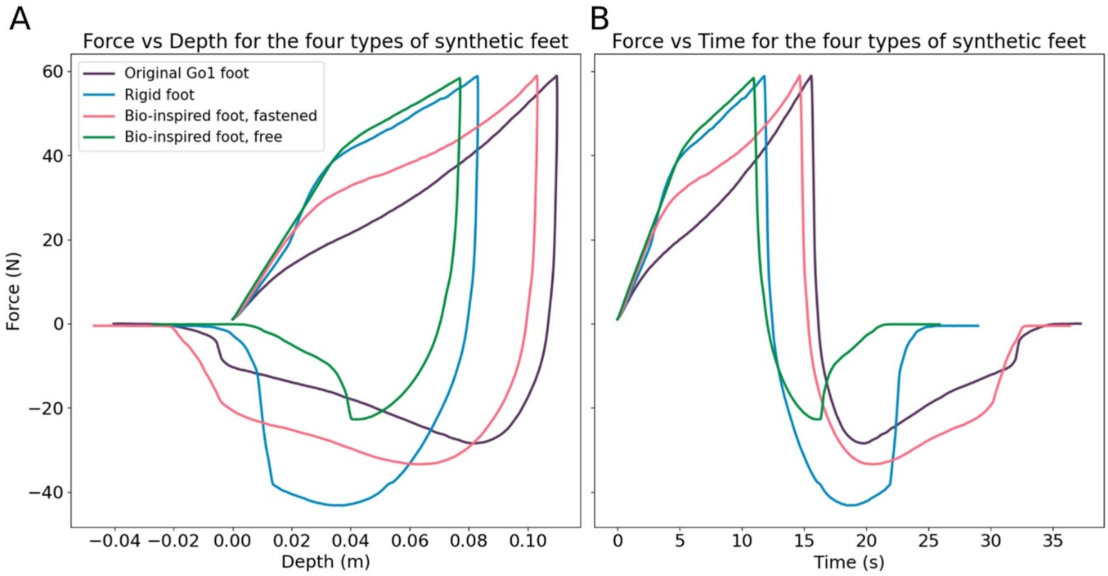

Figure 6. Example curves for the force vs depth relationship (A) and force vs time relationship (B). The examples here are taken from the wettest of the three conditions tested, which is the one best demonstrating all the contributions of the different features of the feet. The curves demonstrate how the three feet have the same effect on mud at the beginning, how some feet reach the force target faster and shallower, and the differences in suction force and their timing, for all the different feet.

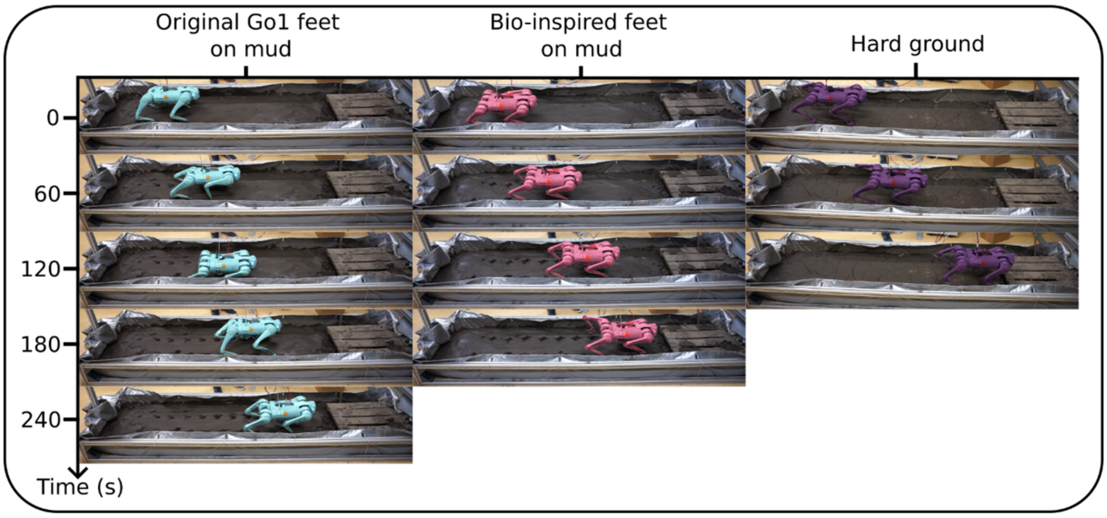

Figure 7. Illustration of the experiments performed with the quadruped Go1. Timeshots of the quadruped walking in the mud using the original Go1 feet or the bio-inspired anisotropic feet and walking on hard ground for comparison. The timeshots demonstrate the different progression speeds of the robot in all three conditions tested. The robot was segmented using segment-anything.com.

robot also is increased using the bio-inspired feet. The speed using the original Go1 feet is 0.83 body length per minute (bl/min), which is similar to our previous research [8], where it was at 0.85 bl min^{-1}. Compared to using the original Go1 feet, the bio-inspired feet enable the robot to progress 55.0% (p-value < 0.01) faster. Figure 8(C) illustrates the footprints left by the quadruped robot after traversing the track, with the original Go1 feet on mud (left), with the bio-inspired anisotropic feet on mud (center), and on hard ground (right).

4. Discussion

Our hypotheses were that split hooves inspired by ungulates have an advantage on wet terrains because they (I) reduce sinkage, (II) reduce suction force, and thereby altogether (III) save energy of locomotion. The summary of the hypotheses results is presented in table 1.

The experiments with the moose feet firmly confirmed the second hypothesis (increase of the suction force at extrusion by 8.4% (p-value < 0.01) and 4.3%

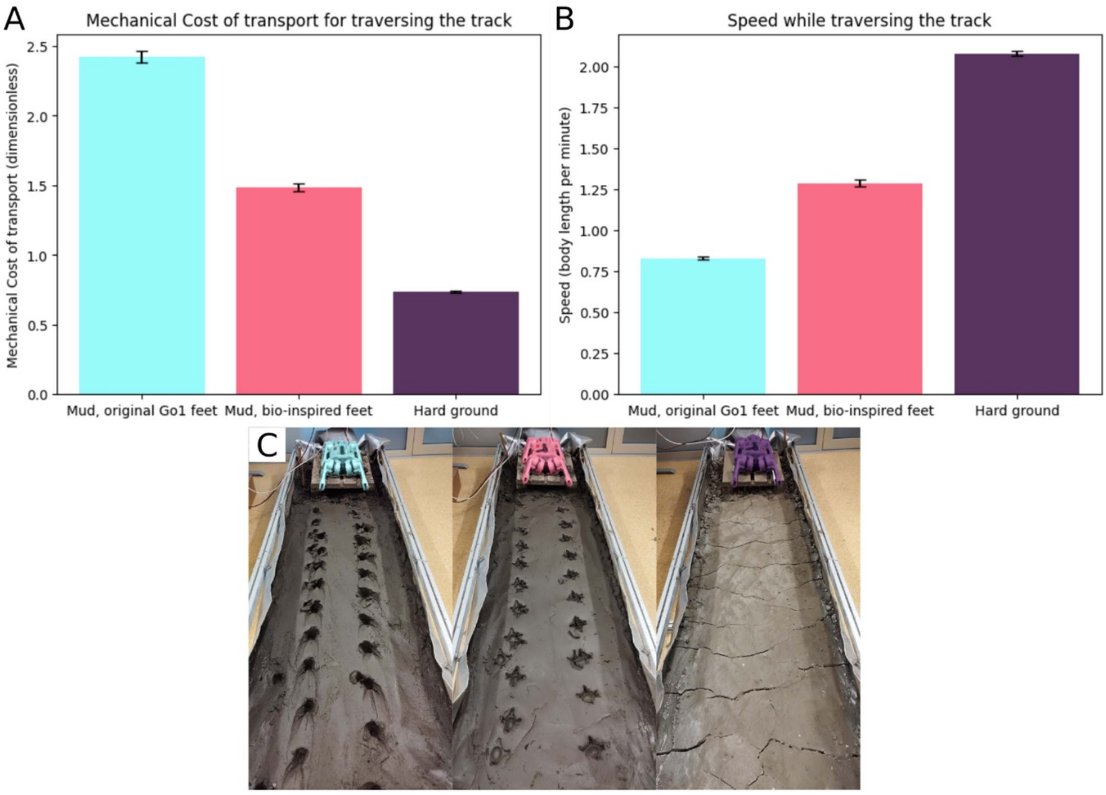

Figure 8. Experimental results with the quadruped robot. The graph shows the difference in Mechanical Cost of Transport (MCoT), speed, and the tracks left by the robot for all three conditions tested. (A) The MCoT of the quadruped while traversing the track filled with mud, while wearing the original Go1 feet, the bio-inspired anisotropic feet, and as a comparison, the same gait on hard ground. (B) The corresponding speed of the quadruped for each experiment. (C) The corresponding tracks left by the robot with original feet on mud (left), with the bio-inspired anisotropic feet on mud (center), and on hard ground (right). The robot was segmented using segment-anything.com. The results reported here represent the median and standard error of a series of 5 runs per condition.

Table 1. Summary of the hypotheses and conclusions from experiments.

	Reduced sinkage (Hypothesis I)	Reduced suction (Hypothesis II)	Saved energy (Hypothesis III)
Moose feet	Inconclusive	Confirmed	Inconclusive
Synthetic feet	Confirmed	Confirmed	Confirmed
Robot	N/A	N/A	Confirmed

(p-value < 0.01) with fastened digits). It also confirms that the effect of suction force is passive as it exists also with the dead animal's feet. Both rear and front feet have the suction force reduction effect. Due to the limitations of the experimental setup, the results were however confirmed only for the water content of 0.34, we therefore cannot confirm that the effect exists or is significant for various mixtures of mud.

The results for the reduced sinkage and energy saving for a moose leg were inconclusive (neither confirmed nor rejected). It could be because the expected effect does not exist, the effect is not passive and cannot be observed with a dead animal or the effect could not be measured because of the restrictions of the experimental setup. The maximum force applied during the experiments was 300 N while the animal weighed about 400 kg, so 1333 N per leg on a tripod gait. The effect may become apparent at larger forces. It is also possible that reduced sinkage is not totally passive because the animal may actively expand the digits during intrusion (our further experiments with synthetic feet indirectly confirm this explanation as the digits of synthetic feet extend passively). Also, our rig allowed only 1D motion whereas the animal might change the orientation of the feet while stepping. Finally, it is possible that sinkage reduction does not play a significant role in ungulate locomotion, or the mechanics are more complicated than what we can observe with passive animal experiments.

For the synthetic ungulate foot inspired design, all three hypotheses were confirmed: the design allowed reducing sinkage, reducing suction force and reducing the overall energy consumption. The rig experiments with synthetic feet were performed on three types of muds with varying water content and the effects were observable in all cases. On mud with low water content, which hardly deforms, the bio-inspired anisotropic foot behaved similarly to the original Go1 foot. Even though percentage-wise the improvements seem huge (reduction of 19.1%, 18.4%, and 82.1% of the energetic cost, sinkage depth, and maximum suction force respectively), the energy, suction force, and work in the almost hard ground are low in absolute values, so the new design of the foot has only marginal benefits with respect to the conventional robot foot design. The real advantage of the ungulate-inspired design becomes apparent with a wet ground where the results were very significant, by all the three metrics we measured (40.3–70.4% of energy saved, 37.4%–46.3% sinkage depth reduction, and 21.0%–47.6% of suction force reduction).

Comparative experiments with variations of the synthetic feet can be used to explain the effects of the design. The rigid extended foot performed even better in the medium water content condition because of its constantly larger surface area, but its static shape does not allow an easy suction force release. Mud on the upper surface of the extended digits also weighs it down. The foot with the fastened digits has the same advantage of reduced suction as the anisotropic foot and the rigid foot in the wettest condition but it sinks deeper. All these behaviors can be visualized on the force vs time and force vs sinkage curves presented in figure 5. There, the original Go1 foot and the foot with fastened digits behave in an equivalent way, as expected. The bio-inspired anisotropic foot and the rigid extended foot, on the other hand, behave also in a similar way to each other during the intrusion phase, but the benefit of the digits' retraction can be well observed when the suction force is quickly released by the bio-inspired anisotropic foot. On the contrary, the rigid foot is impeded by a resistive suction force up to the mud surface, in the same way as the original Go1 foot.

These results complement our previous research [6], where we demonstrated that simply adjusting foot stiffness could increase the force generated by 33% in mud. Our earlier work also highlighted the necessity for an anisotropic design to mitigate suction forces, a challenge we addressed with our bio-inspired anisotropic foot design.

While there appear to be no other studies specifically focused on foot design for locomotion in deep mud, we can draw parallels from research on dry granular materials. For instance [27], found that segmented foot designs reduced sinkage depth by 5% of the leg length in dry sand and pebbles. Similarly [29], also observed that bird-inspired biomechanical feet diminished sinkage in loose sand [25] and [31] reported that larger foot surface areas decreased sinkage depth in various granular materials, noting that in cases of deep sinkage, strong foothold prevents slippage. [30] further indicated that compared to spherical feet, cylindrical feet sink approximately 44% less in dry sand under a static load of 50 N.

Overall, these findings suggest that using larger feet, altering the shape of the feet, or using deformable feet with segments, or made from soft materials, can reduce sinkage in different flowable materials. However, a larger foot, while beneficial in reducing pressure and sinkage, may not be ideal for wet, cohesive materials like mud due to the suction forces that hinder foot liftoff, as demonstrated in [6], and in the current paper. This highlights the necessity of using a deformable foot for locomotion in mud, as was demonstrated in this research.

Finally, the experiments performed on the Go1 quadruped robot confirmed our hypothesis of energy reduction. During locomotion, the MCoT is not only due to the base cost of locomotion, which we measured by performing tests on hard ground, but is also due to the resistive behavior of mud. By comparing the MCoT of the robot through the mud track using both the original Go1 feet, and the bio-inspired anisotropic feet, we established that the latter enabled saving more than half of the energy lost in mud. The reduced sinkage and suction force not only make locomotion easier but also faster, with a significant increase of the locomotion speed of the quadruped using the bio-inspired anisotropic feet, with the same controller. The differences observed in the various settings are only due to the sinkage of the feet and the reduced suction force, which in turn impact the time and energy the robot spends inserting and extruding its feet from the mud and ensuring the robot's stability; the robot speed is not controlled, but instead the increased speed and reduced MCoT emerge from easier locomotion enabled by the feet design.

Overall, our research shows that the bio-inspired anisotropic foot presents several advantages for locomotion on mud. Its passively expanding and retracting digits enable to reduce sinkage, suction force and energetic cost of moving in mud. Also, we cannot think of any use case when these feet would impede locomotion. On hard ground, the passive digits would not touch the ground so they would not disturb foot placement, and at the same time they contribute to energy reduction when the robot is on soft ground. We believe that the advantage exists also on dry yielding grounds such as dry sand or dry snow: reduced sinkage would be reasonable to expect in all yielding grounds whereas the suction force might occur only in case of wet mixtures. Our work also did not address controller design: all robot experiments were performed with a controller for a static gait developed in our previous paper [8]. It is possible that an improved controller design would enhance the effects of wet ground locomotion further or the robot could use different controllers for different substances (e.g. changing water content).

It is also worth noting that besides energy saving the novel foot design also increases the fault-tolerance of the robot (and possibly the survival of an animal). Since it sinks in less and needs less force to get the foot loose, it is less likely to stay stuck.

Finally, it is speculated that split hooves also add stability on uneven terrains so it might play the same effect on robots and could complement the research on the design of more stable feet [13, 27, 32] for soft or uneven grounds. Future work thus can address ungulate locomotion and robot locomotion in versatile yielding and uneven terrains to understand the complicated interaction between mechanical feet design in multiphase environments.

Data availability statement

The data that support the findings of this study are openly available at the following URL/DOI: https://doi.org/10.5281/zenodo.12673097 [40].

Acknowledgment

No animals were killed for the purpose of this study. The legs of the moose were obtained from Nõo Hunting Association, operating under the Estonian Wildlife Management Laws, during the hunting season.

Funding

This work was supported by the European Union's Horizon 2020 research and innovation programme ROBOMINERS under Grant 820971 (G S, K M, R A).

Conflict of interest

Authors declare that they have no competing interests.

Author contributions

Conceptualization: G S, K M, R A. Experimentations: G S. Investigation: G S, K M, R A. Visualization: G S. Funding acquisition: K M. Project administration: K M, R A. Supervision: K M, R A. Writing—original draft: G S, K M Writing—review & editing: G S, K M, R A.

ORCID iDs

S Godon https://orcid.org/0000-0003-1928-2696
A Ristolainen https://orcid.org/0000-0003-3029-9667
M Kruusmaa https://orcid.org/0000-0001-5738-5421

References

[1] Bellicoso C D, Bjelonic M, Wellhausen L, Holtmann K, Günther F, Tranzatto M, Fankhauser P and Hutter M 2018 Advances in real-world applications for legged robots *J. Field Robot.* **35** 1311–26
[2] Mattamala M *et al* 2024 Autonomous forest inventory with legged robots: system design and field deployment (arXiv:2404.14157)
[3] Fan Y, Pei Z, Wang C, Li M, Tang Z and Liu Q 2024 A review of quadruped robots: structure, control, and autonomous motion *Adv. Intell. Syst.* **6** 2300783
[4] Godon S, Kruusmaa M and Ristolainen A 2023 Maneuvering on non-Newtonian fluidic terrain: a survey of animal and bio-inspired robot locomotion techniques on soft yielding grounds *Front. Robot.* AI **10** 1113881
[5] Wong J Y 1989 *Terramechanics and Off-road Vehicles* (Elsevier)
[6] Godon S, Ristolainen A and Kruusmaa M 2022 An insight on mud behavior upon stepping *IEEE Robot. Autom. Lett.* **7** 11039–46
[7] Chen X, Yi J and Shan J 2024 A reduced-order mud reaction force model for robotic foot-mud interactions *2024 IEEE Int. Conf. on Advanced Intelligent Mechatronics (AIM)* (IEEE)
[8] Godon S *et al* 2024 Walking in mud: modelling, control and experiments of quadruped locomotion (https://doi.org/10.36227/techrxiv.172047167.78902329/v1)
[9] Qian F, Zhang T, Korff W, Umbanhowar P B, Full R J and Goldman D I 2015 Principles of appendage design in robots and animals determining terradynamic performance on flowable ground *Bioinspir. Biomim.* **10** 056014
[10] Hosoi A E and Goldman D I 2015 Beneath our feet: strategies for locomotion in granular media *Annu. Rev. Fluid Mech.* **47** 431–53
[11] Zhang T and Goldman D I 2014 The effectiveness of resistive force theory in granular locomotion *Phys. Fluids* **26** 101308
[12] Li C, Zhang T and Goldman D I 2013 A terradynamics of legged locomotion on granular media *Science* **339** 1408–12
[13] Chopra S, Tolley M T and Gravish N 2020 Granular jamming feet enable improved foot-ground interactions for robot mobility on deformable ground *IEEE Robot. Autom. Lett.* **5** 3975–81
[14] Bagheri H, Jayanetti V, Burch H R, Brenner C E, Bethke B R and Marvi H 2023 Mechanics of bipedal and quadrupedal locomotion on dry and wet granular media *J. Field Robot.* **40** 161–72
[15] Slonaker J, Motley D C, Zhang Q, Townsend S, Senatore C, Iagnemma K and Kamrin K 2017 General scaling relations for locomotion in granular media *Phys. Rev.* E **95** 052901
[16] Gkliva R, Remmas W, Godon S, Rebane J, Ochs K, Kruusmaa M and Ristolainen A 2024 A multi-terrain robot prototype with archimedean screw actuators: design, realisation, modelling, and control *IEEE Access* **12** 95820–30
[17] Zhang J, Chen X, Shen W, Song J and Zheng Y 2024 A toe-inspired rigid-flexible coupling wheel design method for improving the terrain adaptability of a sewer robot *Bioinspir. Biomim.* **19** 046003
[18] Lee J, Hwangbo J, Wellhausen L, Koltun V and Hutter M 2020 Learning quadrupedal locomotion over challenging terrain *Sci. Robot.* **5** eabc5986
[19] He J and Gao F 2020 Mechanism, actuation, perception, and control of highly dynamic multilegged robots: a review *Chin. J. Mech. Eng.* **33** 1–30
[20] Lu G, Chen T, Rong X, Zhang G, Bi J, Cao J, Jiang H and Li Y 2023 Whole-body motion planning and control of a quadruped robot for challenging terrain *J. Field Robot.* **40** 1657–77
[21] Choi S, Ji G, Park J, Kim H, Mun J, Lee J H and Hwangbo J 2023 Learning quadrupedal locomotion on deformable terrain *Sci. Robot.* **8** eade2256

[22] Wang C, Zhang R, Dong W, Li T, Jiang L, Xu W, Xu P, Zhou Y and Zou M 2024 Trafficability anticipation for quadruped robot in field operation *J. Field Robot.* **41** 851–66
[23] Su Y, Yang H, Ding L, Xu C, Xu P, Gao H, Niu L, Li W and Liu G 2023 A unified foot–terrain interaction model for legged robots contacting with diverse terrains *IEEE/ASME Trans. Mechatronics* **29** 2661–72
[24] Han Y, Lu Z, Liu G, Zong H, Zhong F, Zhou S and Chen Z 2023 Contact detection with multi-information fusion for quadruped robot locomotion under unstructured terrain *Front. Mech. Eng.* **18** 44
[25] Yao C, Shi G, Xu P, Lyu S, Qiang Z, Zhu Z, Ding L and Jia Z 2024 STAF: interaction-based design and evaluation of sensorized terrain-adaptive foot for legged robot traversing on soft slopes *IEEE/ASME Trans. Mechatronics* (https://doi.org/10.1109/TMECH.2024.3350183)
[26] Ranjan A, Angelini F, Nanayakkara T and Garabini M 2023 Design guidelines for bioinspired adaptive foot for stable interaction with the environment *IEEE/ASME Trans. Mechatronics* **29** 843–55
[27] Chatterjee A *et al* 2023 Multi-segmented adaptive feet for versatile legged locomotion in natural terrain *2023 IEEE Int. Conf. on Robotics and Automation (ICRA)* (IEEE)
[28] Catalano M G, Pollayil M J, Grioli G, Valsecchi G, Kolvenbach H, Hutter M, Bicchi A and Garabini M 2021 Adaptive feet for quadrupedal walkers *IEEE Trans. Robot.* **38** 302–16
[29] Zhang R, Pang H, Wan H, Han D, Li G and Wen L 2020 Design and analysis of the bionic mechanical foot with high trafficability on sand *Appl. Bionics Biomech.* **2020** 3489142
[30] Yang H, Zhang C, Ding L, Wei Q, Gao H, Liu G, Ge L and Deng Z 2024 Comparative study of terramechanics properties of spherical and cylindrical feet for planetary legged robots on deformable terrain *J. Terramech.* **113** 100968
[31] Kolvenbach H *et al* 2021 Traversing steep and granular martian analog slopes with a dynamic quadrupedal robot (arXiv:2106.01974)
[32] Chen G, Qiao L, Zhou Z, Lei X, Zou M, Richter L and Ji A 2024 Biomimetic lizard robot for adapting to Martian surface terrain *Bioinspir. Biomim.* **19** 036005
[33] Liu S, Huang B and Qian F 2023 Adaptation of flipper-mud interactions enables effective terrestrial locomotion on muddy substrates *IEEE Robot. Autom. Lett.* **8** 7978–85
[34] Zhong B, Zhang S, Xu M, Zhou Y, Fang T and Li W 2018 On a CPG-based hexapod robot: amphiHex-II with variable stiffness legs *IEEE/ASME Trans. Mechatronics* **23** 542–51
[35] Ren X *et al* 2013 An experimental study on the locomotion performance of elliptic-curve leg in muddy terrain *2013 IEEE/ASME Int. Conf. on Advanced Intelligent Mechatronics* (IEEE)
[36] Raibert M, Blankespoor K, Nelson G and Playter R 2008 Bigdog, the rough-terrain quadruped robot *IFAC Proc. Vol.* **41** 10822–5
[37] Phillips C J C and Morris I D 2000 The locomotion of dairy cows on concrete floors that are dry, wet, or covered with a slurry of excreta *J. Dairy Sci.* **83** 1767–72
[38] Abad S-A, Sornkarn N and Nanayakkara T 2016 The role of morphological computation of the goat hoof in slip reduction *2016 IEEE/RSJ Int. Conf. on Intelligent Robots and Systems (IROS)* (IEEE)
[39] Gkliva R and Kruusmaa M 2022 Soft fluidic actuator for locomotion in multi-phase environments *IEEE Robot. Autom. Lett.* **7** 10462–9
[40] Godon S, Ristolainen A and Kruusmaa M 2024 Dataset for the article: robotic feet modeled after ungulates improve locomotion on soft wet grounds *Zenodo* (https://doi.org/10.5281/zenodo.12673097)